Research Article

Combination of epidural electrical stimulation with *ex vivo* triple gene therapy for spinal cord injury: a proof of principle study

https://doi.org/10.4103/1673-5374.293150

Received: October 15, 2019

Peer review started: November 3, 2019

Accepted: April 29, 2020

Published online: September 22, 2020

Filip Olegovich Fadeev[1], Farid Vagizovich Bashirov[1], Vahe Arshaluysovich Markosyan[1], Andrey Alexandrovich Izmailov[1], Tatyana Vyacheslavovna Povysheva[1], Mikhail Evgenyevich Sokolov[1], Maxim Sergeevich Kuznetsov[1], Anton Alexandrovich Eremeev[2], Ilnur Ildusovich Salafutdinov[2], Albert Anatolyevich Rizvanov[2], Hyun Joon Lee[3, 4, *], Rustem Robertovich Islamov[1, *]

Abstract

Despite emerging contemporary biotechnological methods such as gene- and stem cell-based therapy, there are no clinically established therapeutic strategies for neural regeneration after spinal cord injury. Our previous studies have demonstrated that transplantation of genetically engineered human umbilical cord blood mononuclear cells producing three recombinant therapeutic molecules, including vascular endothelial growth factor (VEGF), glial cell-line derived neurotrophic factor (GDNF), and neural cell adhesion molecule (NCAM) can improve morpho-functional recovery of injured spinal cord in rats and mini-pigs. To investigate the efficacy of human umbilical cord blood mononuclear cells-mediated triple-gene therapy combined with epidural electrical stimulation in the treatment of spinal cord injury, in this study, rats with moderate spinal cord contusion injury were intrathecally infused with human umbilical cord blood mononuclear cells expressing recombinant genes *VEGF165*, *GDNF*, *NCAM1* at 4 hours after spinal cord injury. Three days after injury, epidural stimulations were given simultaneously above the lesion site at C5 (to stimulate the cervical network related to forelimb functions) and below the lesion site at L2 (to activate the central pattern generators) every other day for 4 weeks. Rats subjected to the combined treatment showed a limited functional improvement of the knee joint, high preservation of muscle fiber area in tibialis anterior muscle and increased H/M ratio in gastrocnemius muscle 30 days after spinal cord injury. However, beneficial cellular outcomes such as reduced apoptosis and increased sparing of the gray and white matters, and enhanced expression of heat shock and synaptic proteins were found in rats with spinal cord injury subjected to the combined epidural electrical stimulation with gene therapy. This study presents the first proof of principle study of combination of the multisite epidural electrical stimulation with *ex vivo* triple gene therapy (*VEGF*, *GDNF* and *NCAM*) for treatment of spinal cord injury in rat models. The animal protocols were approved by the Kazan State Medical University Animal Care and Use Committee (approval No. 2.20.02.18) on February 20, 2018.

Key Words: adenoviral vector; epidural electrical stimulation; gene therapy; glial cell-line derived neurotrophic factor; human umbilical cord blood mononuclear cell; neural cell adhesion molecule; spinal cord injury; vascular endothelial growth factor

Chinese Library Classification No. R445; R364; R741

Introduction

Spinal cord injury (SCI) results in massive loss of neurons and glial cells at the site of damage immediately after the injury. In addition, post-traumatic cell loss followed by acute nerve cell death expands beyond the injury epicenter and persists for several days and even weeks (Wilson et al., 2013). This secondary lesion may affect undamaged neural circuitries away from the lesion site when long-distance axons of supraspinal or intraspinal neurons are damaged. As an example, the disruption of corticospinal axons at the site of SCI resulted in death of spinal motoneurons below the level of injury followed by progressive atrophy in skeletal muscle fibers which may have been innervated by those cortical axons and spinal motoneurons (Zhang et al., 2018).

Three main categories of interventions are often suggested as potential treatments for SCI (Hamid and Hayek, 2008):

[1]Department of Medical Biology and Genetics, Kazan State Medical University, Kazan, Russia; [2]Institute of Fundamental Medicine and Biology, Kazan [Volga Region] Federal University, Kazan, Russia; [3]Department of Neurology, University of Mississippi Medical Center, Jackson, MS, USA; [4]Research Service, G.V. (Sonny) Montgomery VA Medical Center, Jackson, MS, USA

*__Correspondence to:__ Hyun Joon Lee, PhD, hlee@umc.edu; Rustem Robertovich Islamov, MD, Dr.Sci., rustem.islamov@gmail.com.
https://orcid.org/0000-0002-6985-0690 (Hyun Joon Lee); https://orcid.org/0000-0002-6632-4636 (Rustem Robertovich Islamov)

Funding: *This study was supported by the grant of Russian Science Foundation, No. 16-15-00010 (to RRI). AAR was supported by the Russian Government Program of Competitive Growth of Kazan Federal University.*

How to cite this article: *Fadeev FO, Bashirov FV, Markosyan VA, Izmailov AA, Povysheva TV, Sokolov ME, Kuznetsov MS, Eremeev AA, Salafutdinov II, Rizvanov AA, Lee HJ, Islamov RR (2021) Combination of epidural electrical stimulation with ex vivo triple gene therapy for spinal cord injury: a proof of principle study. Neural Regen Res 16(3):550-560.*

(1) pharmacological agents that prevent the secondary damages and stabilize the injured spinal cord during the post-traumatic spinal shock, (2) gene and cell therapy to stimulate neuroregeneration at the site of lesion, and (3) electrical stimulations to reactivate central pattern generators below the level of injury.

Percutaneous electrical stimulation of nerve endings has been commonly used in sports medicine and rehabilitation for patients with neurotrauma or diseases in the neuromuscular system. Numerous preclinical and clinical studies have shown beneficial effects of electrical stimulations to the spinal cord dura mater after traumatic injury (Martin et al., 2012; Ho et al., 2014). Electrical stimulations benefit for each motor component— motoneurons and muscle fibers. Post-traumatic electrical stimulation of the spinal cord has been shown to increase the viability of the preserved spinal neurons and prevents their degeneration (Zhang et al., 2018). The neuroprotective effects of exogenous electric current on preserved neurons appear to be associated with activation of various signaling molecules and their corresponding intracellular cascades. Calcium influx through the L-voltage-sensitive Ca^{2+} channels results in the rise of intracellular Ca^{2+} level that activates the well-known cytoplasmic signaling molecules, such as phospholipases, protein-kinase C, and phosphoinositide 3-kinase (PI3K) (Clapham, 2007). Subsequently, the Ca^{2+} induced intracellular signals activate cAMP response element-binding protein (CREB) (West et al., 2001), nuclear factor kappa-light-chain-enhancer of activated B cells (NF-κB) (Lilienbaum and Israël, 2003), mitogen-activated protein kinases/extracellular signal-regulated kinases (MAPK/ERK) (Wiegert and Bading, 2011) and phosphatidylinositol 3-kinase/protein kinase B (PI3K/Akt) (Leinninger et al., 2004; Zhong, 2016) pathways that regulate the expression of genes encoding neurotrophic factors like brain derived neurotrophic factor (Wenjin et al., 2011) and neurotrophin-3 (Zhang et al., 2017).

Epidural electrical stimulation (EES) of the spinal cord is a potential neurorehabilitation method for spinal cord injury. EES of lumbosacral spinal cord has been shown to activate spinal locomotor networks such as central pattern generator and enable standing and stepping in spinalized animals (Ichiyama et al., 2005; Lavrov et al., 2006) and patients with SCI (Gill et al., 2018; Taccola et al., 2018).

The multisite EES that applies electrical stimulations at multiple levels across the post-traumatic spinal cord has been suggested to facilitate the activation of various neuronal networks relevant to impaired functions. For instance, a concurrent neuromodulation of sensory pathways along with motor network activation has been shown to provide the synergistic motor performance in neurorehabilitation after SCI (Gerasimenko et al., 2015; Shah and Lavrov, 2017).

The gene therapy after SCI is considered a therapeutic strategy that may enhance the survival of preserved nerve cells and promote neuronal regeneration (Hamid and Hayek, 2008; Walthers and Seidlits, 2015). Direct (*in vivo*) gene therapy has mostly focused on the delivery of recombinant genes encoding neurotrophic, anti-apoptotic, and anti-inflammatory molecules to the site of lesion (Walthers and Seidlits, 2015). To date, several gene therapies have been developed in preclinical studies and advanced to clinical trials in neurodegenerative diseases such as amyotrophic lateral sclerosis (Zavalishin et al., 2008), Alzheimer's and Parkinson's diseases (Rafii et al., 2014; Warren Olanow et al., 2015). Recently, we have demonstrated that an intrathecal infusion of human umbilical cord blood mononuclear cells (UCBMCs) transduced with adenoviral vectors carrying genes encoding vascular endothelial growth factor (VEGF), glial cell-line derived neurotrophic factor (GDNF) and neural cell adhesion molecule (NCAM) successfully promoted neuronal protection in rats and mini-pigs following SCI (Islamov et al., 2017; Izmailov et al., 2017a). Preclinical studies have demonstrated that cell-mediated (*ex vivo*) gene therapy using genetically engineered cells has at least two advantages: (1) the direct exposure of viral vector to the recipients, which may cause toxic and immunogenic effects in *in vivo* gene therapy, can be significantly reduced; and (2) the production of recombinant molecules can be controlled via the regulation of viral transduction levels in host cells and via the regulation of numbers of the genetically engineered cells for transplantation (Lim et al., 2010). To enhance the first advantage, adenoviral vectors of the second generation have been used in the current studies (Islamov et al., 2015). Investigation of the safety of UCB cell transplantation in different human populations with SCI has entered the early phase clinical trials (Ichim et al., 2010; Liu et al., 2013; Yao et al., 2013; Zhu et al., 2016).

This study was designed to evaluate the therapeutic efficacy of combined multisite EES with gene therapy on SCI in rat models.

Materials and Methods

Animals

Experiments were performed in female Wistar rats (7 months old, 250–300 g; Pushchino Laboratory, Pushchino, Russia). Female rats were chosen for the ease and consistency of manual bladder emptying achievable in the acute phase after SCI due, in part, to their anatomical characteristics. An inconsistent or incomplete bladder emptying may negatively affect the assessment of locomotor function, joint kinematics, and electrophysiology. In addition, the use of female rats allowed us to compare results from this study with our previous report (Izmailov et al., 2017a). Rats were housed according to approved procedures for the use of animals in laboratory experiments. The animal protocols were approved by the Kazan State Medical University Animal Care and Use Committee (approval No. 2.20.02.18) on February 20, 2018. The number of animals was determined based on pioneer exploratory investigations on multisite EES and gene therapy, each of which has already advanced to clinical trials (Rafii et al., 2014; Warren Olanow et al., 2015; Gill et al., 2018).

Adenoviral vectors and gene engineered human UCBMCs

Preparation of recombinant adenoviral vectors

Second-generation adenoviral vectors carrying human *VEGF165*, *GDNF*, *NCAM1* genes or green fluorescent protein (GFP) were produced in Scientific Research Institute of Epidemiology and Microbiology named after N. F. Gamalei (Moscow, Russia) as described previously (Islamov et al., 2015). The nucleotide sequences encoding *VEGF165* (Gene BankNM 001171626.1), *GDNF* (Gene Bank NM 019139.1) and *NCAM1* (Gene Bank NM 001076682.2) were obtained by chemical synthesis (Evrogen Joint Stock Company, Moscow, Russia). In short, the target genes were cloned into a shuttle plasmid vector pShuttle-CMV (Stratagene, La Jolla, CA, USA). The adenoviral vectors, Ad5-*VEGF*, Ad5-*GDNF*, Ad5-*NCAM*, and Ad5-*gfp* were obtained by the method of homologous recombination in E. coli strain BJ5183 cells (Stratagene), grown in HEK-293 cell culture and purified by exclusion chromatography (Peng et al., 2006). The titers of Ad5-*VEGF* (1.8×10^9 PFU/mL), Ad5-*GDNF* (2.0×10^9 PFU/mL) and Ad5-*NCAM* (2.2×10^9 PFU/mL) were determined by the plaque formation technique in the HEK-293 cell culture (Mittereder et al., 1996).

Preparation of gene engineered hUCBMCs

UCB was taken after obtaining informed consent of the pregnant and prenatal screening for contraindications to blood donation. All manipulations were performed in accordance with the protocol of the legitimate and ethical standards

generally accepted in the stem cell bank of the Kazan State Medical University (FS-16-01-001450) on December 26, 2017. Mononuclear fraction of UCB was isolated by the standard procedure of sedimentation onto a density barrier. In short, 50 mL of tube was sequentially added with 25 mL of Ficoll solution with a density of 1.077 g/mL (PanEko, Moscow, Russia), to which an equal volume of UCB with anticoagulant was carefully layered. After centrifugation at 720 × *g* for 20 minutes, leukocyte fraction was collected into a separate tube, resuspended in Dulbecco's phosphate-buffered saline (DPBS, PanEco) at a ratio of 1:2 and centrifuged at 305 × *g* for 15 minutes. The resulted cell pellets were resuspended in 10 mL of DPBS and again centrifuged at 305 × *g* for 15 minutes. To remove red blood cells, cell pellets were resuspended in a hypotonic cell lysis buffer (0.168 M NH_4Cl, 0.1 M $KHCO_3$, 1.27 mM ethylenediaminetetraacetic acid, pH 7.3) and washed with DPBS solution. The obtained fraction of mononuclear cells was cultivated in RPMI-1640 medium (Sigma, St. Louis, MO, USA) supplemented with 10% fetal bovine serum (FBS) and a mixture of antibiotics penicillin and streptomycin (100 U/mL, 100 μg/mL).

The transduction of UCBMCs was performed as described in our established protocol (Islamov et al., 2015). The cells were simultaneously transduced with three adenoviral vectors at an equal ratio: Ad5-*VEGF* (1/3) + Ad5-*GDNF* (1/3) + Ad5-*NCAM* (1/3) or with Ad5 carrying *gfp*. The total multiplicity of infection (MOI) was 10. For xenotransplantation, two million modified cells (UCB-MC + Ad5-*VEGF*/*GDNF*/*NCAM*) were prepared in 20 μL of saline per injection. The efficacy of UCB-MC transduction with therapeutic genes was confirmed by real-time PCR as described previously (Islamov et al., 2015).

ELISA: GDNF, VEGF, and NCAM protein assay

With sandwich enzyme-linked immunosorbent assay (ELISA) kits (R&D Systems, Minneapolis, MN, USA), the levels of soluble recombinant human VEGF, GDNF and NCAM were estimated in the conditioned culture media from the culture of UCBMCs transduced with Ad5-*VEGF*, Ad5-*GDNF*, and Ad5-*NCAM*. UCBMCs transduced with Ad5-*gfp* alone served as a control. Naïve and genetically engineered UCBMCs were incubated in RPMI-1640 medium (PanEco) containing 10% FBS at 37°C under 5% CO_2. After 72 hours of incubation, conditioned culture media were collected, centrifuged at 4°C at 1000 × *g* for 10 minutes and stored at –80°C before use. The levels of VEGF165, GDNF and NCAM1 were determined in supernatants using Human VEGF DuoSet ELISA kit (Cat# DY293B), Human GDNF DuoSet ELISA kit (Cat# DY212) and Human NCAM-1/CD56 DuoSet ELISA kit (Cat# DY2408). Concentrations of VEGF, GDNF, and NCAM were determined according to the manufacturer's instructions.

Surgery and post-operative care

Animals were anesthetized with a mixture of Zoletil 100 (3 mg/kg; Virbac Laboritaries, Val de Reuil, France) and Xyla (4.8 mg/kg; Interchemie werken "De Adelaar B.V", Venray, Netherlands) administered by intraperitoneal injection. All surgical procedures were performed under aseptic conditions and were divided into three stages (**Figure 1**):

(1) Implantation of stimulating electrodes. This stage included an installation of a 12-pin headplug (Omnetics Connector Corporation, Minneapolis, MN, USA) and teflon-coated wire electrodes (AS632, Cooner Wire Company, Chatsworth, CA, USA) to connect an EES stimulator to electrodes on the headplug (Lavrov et al., 2008). Stimulating electrodes were placed at C5 and at L2 before SCI at T8–9 level. After local laminectomy at C5 and L2 levels, the electrodes were tied to the dura mater using 9.0 suture. The wires of the headplug were routed under the skin. In previous studies regarding EES on animals, stimulating electrodes were implanted at various time points before, during, or after SCI (Ichiyama et al., 2005; Lavrov et al., 2006; Thornton et al., 2018). In the current study, we implanted stimulating electrodes before SCI to minimize potential surgical complications affecting evaluation of locomotor recovery post SCI, avoid losing experimental animals during the electrode implantation surgery, and include only animals with successful headplug implantation resulting in muscle contractions.

(2) SCI. Contusion SCI was induced 1 week after implantation of electrodes in a standard way as described previously (Mukhamedshina et al., 2016; Izmailov et al., 2017a). A mid-dorsal skin incision was made from vertebrae T7–10, tendons and muscles were removed from the spinous processes and vertebral arches and laminectomy was performed at the T8–9 vertebral level. Contusion SCI was induced using an impact rod (weight 10 g, diameter 2 mm) centered above T8 and dropped from a height of 25 mm onto the exposed dura mater of the spinal cord, which inflicts a moderate contusion injury (Lebedev et al., 2008). Before closing the wound, two surgeons verified the contusion injury according to the appearance of hematoma at the site exposed to the impact rod.

(3) Gene therapy (xenotransplantation of genetically modified human UCBMCs). A proper level of anesthesia was maintained for 4 hours after modeling of SCI (supplemental doses of Zoletil administered, i.p. as needed). While rats were kept under anesthesia, their body temperature was maintained at 37–38°C with a heating pad. After 4 hours, animals underwent a laminectomy at the level of L4–5. Intrathecal injection of 20 μL of solution was made using a 25-μL Hamilton syringe and a 33 gauge needle. Five animals with implanted stimulating electrodes received 2 × 10^6 human UCBMCs and Ad5-*VEGF*/GDNF/*NCAM* in 20 μL of saline prepared as described above. Ten rats after implantation of stimulating electrodes were injected with 20 μL of saline.

After surgery, all rats received post-operative care to reduce suffering and distress. Animals were daily injected intramuscularly for 5 days with antibiotic Ceftriaxone (50 mg/kg, Sandoz, Austria) and anesthetic Ketamin (2.5 mg/kg, Dr. Reddy's Laboratories, Ltd., Hyderabad, Andhra Pradesh, India). The bladder and colon were manually emptied until spontaneous voiding returned. The health condition of rats was assessed daily for 30 days after SCI based on the progress of wound healing, the vital signs like rectal temperature and respiration rate, the ability to access food or water and body weight.

All 15 rats with SCI survived till the end of the investigation and were euthanized under anesthesia in accordance with the criteria for euthanasia and humane end points. On the 30th day of the experiment, animals for histological assessment were deeply anesthetized with intraperitoneal injection of sodium pentobarbital (60 mg/kg; Sigma). The duration of the experiment was established based on our previous studies that demonstrated the morpho-functional recovery of rat spinal cord in this moderate SCI model (Mukhamedshina et al., 2016).

Epidural electrical stimulation

Epidural electrical stimulation (EES) was performed with Digitimer DS5 (Digitimer Ltd., Welwyn Garden City, UK) and stimulation parameters (40 Hz, 1.3–2 V and 0.2 ms pulse duration) were controlled using LabChart data acquisition and analysis system (AD Instruments Inc., Sydney, Australia). EES procedure was started 3 days after SCI and was performed above the lesion site at C5 (to stimulate cervical network related with forelimb functions) and below the injury at L2 (to activate central pattern generators) (Shah and Lavrov, 2017). The stimulation was applied simultaneously at both C5 and L2 vertebral levels. The procedure was performed for 30 minutes in the morning and 30 minutes in the evening every other

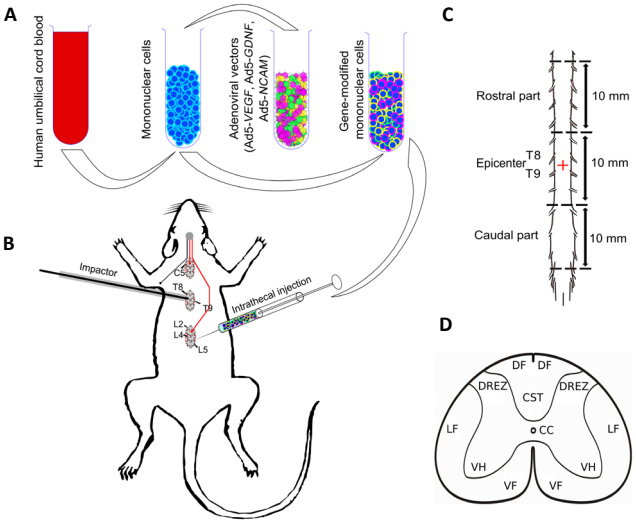

Figure 1 | **Experimental design.**
(A) Preparation of gene engendered human umbilical cord blood mononuclear cells (UCBMCs) expressing recombinant VEGF, GDNF, and NCAM. (B) Spinal cord injury (SCI), intrathecal injection of UCBMCs + Ad5-*VEGF*/*GDNF*/*NCAM* 4 hours after surgery, epidural electrical stimulation at C5 and L2 vertebral levels 3 days after SCI. (C) For histological study, spinal cord fragment (30 mm) was divided in three segments: the injury epicenter (10 mm) in the middle and two segments rostral (10 mm) and caudal (10 mm) to the epicenter. (D) Spinal cord zones used for immunofluorescence staining and morphometric analysis. Seven spinal cord areas were selected: ventral horn (VH), ventral corticospinal tract (CST), dorsal root entry zone (DREZ), area of the central canal (CC), dorsal funiculi (DF), ventral funiculi (VF), outer area of the lateral funiculi at the line passing through the central canal (LF). GDNF: Glial cell-line derived neurotrophic factor; NCAM: neural cell adhesion molecule; VEGF: vascular endothelial growth factor.

day for 4 weeks after SCI. During EES, rats were placed on a treadmill running at a fixed speed of 10 cm/s. The animals were secured in a body-weight supporting harness system at an angle of approximately 45° so that only hindlimbs were placed on the treadmill surface and rats were able to make steps (Ichiyama et al., 2008). The patterns of stimulation and the treadmill training were constant throughout the experiment. Hence, treadmill training and EES stimulation were performed simultaneously.

Experimental groups

In this study, animals were divided into four experimental groups: (1) intact, healthy rats (I group, n = 6); (2) control rats with SCI were intrathecally injected with 20 µL of saline (C group, n = 6); (3) rats with SCI were intrathecally injected with 20 µL of saline and underwent EES during treadmill training (ES group, n = 4); and (4) rats with SCI received gene therapy (infusion of 2 × 10^6 gene modified UCBMCs in 20 µL of saline) and EES during treadmill training (GT + ES group, n = 5). It is important to note that the design of the experiment did not include a group of rats with SCI treated only with UCBMCs and Ad5-*VEGF*/*GDNF*/*NCAM*, as they have previously shown a positive effect of on neuroregeneration after the same SCI (Izmailov et al., 2017a).

Assessment of joint kinematics

Functional recovery was assessed on the 30th day after SCI by evaluation of the kinematics of the hindlimb. The color marks were plotted in the projection of the iliac crest, of the greater trochanter of the femur, of the knee and ankle joints, and of the fingers on the left sides (Courtine et al., 2008). Rats were placed in a body-weight supporting harness system and placed on a treadmill running at a speed of 10 cm/s. Video recording of the color marks during rats walking on a treadmill was carried out using a Canon Power Shot S5 IS camera (Tokyo, Japan). The obtained video records of five step cycles were used to determine the angles from the hip, knee and ankle joints. The range of motion was calculated as the difference between the maximal and minimal angles of each joint. Video analysis of joint kinematics was carried out using Software Kinovea 0.8.23 (Harvie et al., 2017).

Electrophysiological study

Electrophysiological evaluation of motor function recovery was done 30 days after SCI. The electromyography (EMG) of the medial head of gastrocnemius muscle was evoked by electrical stimulations of the sciatic nerve (n. ischiadicus). EMG recording was performed subsequently at each hindlimb on both left and right sides of animals. Stimulations were composed of rectangular impulses (one stimulus every 2 minutes) with a duration of 0.5 ms. The stimulus intensity was incrementally increased from 0.3 to 30 V to determine the threshold voltage. The 5 Hz high pass and 2 kHz low pass filters were used. The threshold, amplitude, and the latency of H reflex (monosynaptic reflex) from spinal motoneurons and the motor (M) response from medial gastrocnemius muscles were measured. The ratio of maximal sizes of H- and M-responses (H/M ratio = [H_{max}/M_{max}] × 100%) was calculated (Lee et al., 2009). To generate electrical pulses as well as to amplify and record the EMG responses, electromiographer MG-42 (Medicor, Budapest, Hungary) was used.

Histological study

For histological investigation, animals were sacrificed after the terminal experiments on the 30th day post-operation. Injury epicenter segments were used for the investigation of regenerating myelinated fibers in the white matter of the spinal cord. Segments caudal to the epicenter were used for studies of gray matter sparing and immunofluorescent analysis to investigate molecular and cellular changes in the spinal cord after contusion injury.

Animals were deeply anesthetized by intraperitoneal injection of sodium pentobarbital (60 mg/kg) and intracardially perfused with 4% paraformaldehyde (Sigma) in phosphate-buffered saline (PBS, pH 7.4). Spinal cord tissues (30 mm) centered at contusion site were harvested and cut into three segments: the injury epicenter (10 mm) in the middle and two segments rostral (10 mm) and caudal (10 mm) to the epicenter (**Figure 1C**). Rostral and caudal segments were post-fixed in 4% paraformaldehyde at 4°C overnight and prepared for immunofluorescent staining. The segments at the epicenter were post-fixed in 2.5% glutaraldehyde for 4 hours, incubated in 1% osmium tetroxide for 24 hours and embedded in EMbed 812 (Electron Microscopy Sciences, Hatfield, Pennsylvania) for morphometric analysis.

Three segments of the spinal cord (rostral, epicenter, and caudal) were processed to evaluate the combinatorial effect of EES and gene therapy on neuroregeneration. The rostral segment was used for analysis of the transplanted UCBMCs and Ad5-*VEGF*/*GDNF*/*NCAM* (their migratory potential, survivability, and production of the recombinant molecules VEGF, GDNF, and NCAM). The segments centered at the epicenter were used to analyze sparing of the white matter and the regeneration of axons through the epicenter of injury toward the caudal segment. The caudal segment with moderate damages was used to evaluate the efficacy of neural reconstruction below the injury in terms of sparing of the gray matter, molecular changes, and cellular responses.

Skeletal muscles, tibialis anterior and medial head of gastrocnemius, were harvested in all experimental animals from both hindlimbs and frozen cross sections were prepared for hematoxylin and eosin staining.

Morphometric analysis

The resin-embedded epicenter segments were cut in the

middle and the caudal half segments were used to estimate white matter sparing (**Figure 1C**). Cross semi-thin sections were obtained from both rostral and caudal ends of the segment at a distance of 5 mm from each other and stained with methylene blue dye. Preservation of the white matter was examined in squares (0.08 mm^2) at the ventral, lateral, and dorsal columns at both sides of the spinal cord. The number of myelinated fibers was counted with the AxioVision Rel. 4.8. Software (Carl Zeiss, Oberkochen, Germany).

Preservation of gray matter was investigated in caudal segments (**Figure 1C**). Frozen spinal cord cross sections were collected at the rostral end of caudal segments at an interval of 50 µm over 0.5 mm-long spinal cord (totally 10 sections) and were subjected to hematoxylin and eosin staining. The total area of the gray matter and the cystic cavities area were measured using Image J Software (National Institutes of Health, Bethesda, Maryland, USA). The obtained results were converted into percent values.

The mean area of the tibialis anterior and medial gastrocnemius skeletal muscle fibers was measured using Image J Software (National Institutes of Health, Bethesda, MD, USA). Two hundred muscle fibers were evaluated from each muscle.

Immunofluorescence staining

Free-floating cross sections (20 µm-thick) were obtained from rostral and caudal segments with a cryostat (Microm HM 560, Thermo Scientific, Waltham, MA, USA). Rostral segment above the injury epicenter was employed to investigate the migration potential, survivability, and efficacy of gene expression in transplanted UCBMCs (**Figure 1C**). Anti-HNA antibodies were used for identification of human UCBMCs in the rat spinal cord. Double immunofluorescence staining with the HNA antibody and antibodies to each human recombinant molecule (VEGF, GDNF, NCAM) was employed to analyze the expression of those genes in UCBMCs (**Table 1**). Caudal segment below the injury epicenter with moderate post-traumatic changes was selected to evaluate cellular and molecular changes in post-traumatic spinal cord with and without combined electrical stimulation and gene therapy. Survivability of spinal cord cells was evaluated using Abs to proapoptotic Caspase3 and stress Hsp27 proteins. Synaptic function of preserved neurons was assessed with Abs against synaptophysin and PSD95 (**Table 1**). Nuclear counterstaining was performed with DAPI (10 µg/mL in PBS; Sigma).

Immunofluorescence labeling of spinal cord cells and UCBMCs was evaluated in the ventral horns (VH), dorsal root entry zone (DREZ), area around the central canal (CC), main corticospinal tract (CST), and ventral, dorsal and lateral funiculi (VF, DF and LF) (**Figure 1D**). Images were taken with the LSM 510-Meta microscope (Carl Zeiss; Oberkochen, Germany). The number of Caspase3-immunopositive cells was counted by nuclear counterstaining with 4',6-diamidino-2-phenylindole from 10 adjacent optical slices in area of 0.05 mm^2. The immunoexpression levels of Hsp27, synaptophysin, and PSD95 were estimated according to the fluorescence density of the corresponding markers in area of 0.05 mm^2. Digital fluorescence images were visually assessed using Zen 2012 Software (Carl Zeiss, Oberkochen, Germany) and mean intensities were calculated (Izmailov et al., 2017a).

Statistical analyses

All steps of data processing and analysis were performed in R Environment for Statistical Computing version 3.4.4 (R Foundation for Statistical Computing, Vienna, Austria) using some additional packages from CRAN repository (https://cran.r-project.org/): ggplot2, dplyr and PMCMRplus. Descriptive statistics are presented as a median [minimum, maximum]. To visualize sample distributions, we used boxplots in combination with scatter plots to represent individual observations. To analyze all the obtained numerical data in behavioral tests, morphometrics, and immunofluorescence assays, we used Kruskal-Wallis test, then in case of null-hypothesis was rejected ($P_{obs} < 0.05$), pairwise comparisons were performed using Dunn's test with Holm adjustment procedure, $P_{adj} < 0.05$ was used as a cut-off for statistically significant results). All tests with animals, morphometric and statistical analyses with respect to the experimental groups were performed in a "blinded" manner.

Table 1 | **Primary and secondary antibodies used in immunofluorescence staining**

Antibody	Host	Dilution	Source
Caspase3	Rabbit	1:200	Abcam (ab2302)
GDNF	Rabbit	1:100	Santa Cruz (sc-328)
HNA	Mouse	1:150	Millipore (MAB1281)
Hsp27	Rabbit	1:200	Abcam (ab12351)
NCAM	Rabbit	1:100	Abcam (ab204446)
PSD95	Rabbit	1:200	Abcam (ab18258)
Synaptophysin	Rabbit	1:200	Abcam (ab14692)
VEGF	Rabbit	1:200	Santa Cruz (sc-507)
Anti-mouse IgG conjugated with Alexa 488	Donkey	1:200	Invitrogen (A32766TR)
Anti-rabbit IgG conjugated with Alexa 647	Donkey	1:200	Invitrogen (A32795)
Anti-rabbit IgG (Texas Red) preadsorbed	Donkey	1:200	Abcam (ab7081)

GDNF: Glial cell-line derived neurotrophic factor; HNA: human nuclear antigen; Hsp27: heat shock protein 27 kDa; NCAM: neural cell adhesion molecule; PSD95: postsynaptic density protein 95 kDa; VEGF: vascular endothelial growth factor.

Results

General behavior evaluation

During EES sessions throughout the experiments, rats in the ES group showed signs of spasticity such as spontaneous kicking and uncoordinated, unilateral hindlimb movements which became less frequent at the terminal procedure on the 30th day after SCI. In contrast, animals in the GT + ES group demonstrated less pronounced signs of spastic movements, which disappeared at later sessions of the EES.

During EES sessions in animals in both ES and GT + ES groups, evoked micturition was observed. It is important to note that animals with SCI from all experimental (C, ES and GT + ES) groups were not able to void voluntarily due to urinary incontinence. To empty the bladder, we resorted to a standard procedure of expressing the bladder (Crede maneuver). In the C and ES groups, animals underwent the bladder expression procedure until they regain voluntary micturition usually by 12–14 days after injury. In the GT + ES group, however, reestablishment of voluntary micturition was observed as early as 9–10 days after SCI. Taken all together, these general behavior observations demonstrated better performances i.e. fewer spastic movements and earlier recovery of micturition in rats in the GT + ES group compared to control groups.

Functional recovery

Evaluation of hindlimb function recovery in rats with SCI was performed on the 30th day post-operation. The volumetric analysis of movements of the hip, knee, and ankle joints and the EMG analysis of the gastrocnemius muscle were compared.

Hindlimb locomotor recovery

The skeletal muscles that move the hip and knee joints were innervated by spinal motoneurons of the lumbar plexus (LI–LIV), and the skeletal muscles of the ankles are innervated by motoneurons of the sacral plexus (LIV–LVI) (Gerfen and Paxinos, 2004). Both nervous plexuses originate from the

spinal cord level below the injury epicenter at T8–9. In this study, the volumetric movements of the hip and ankle joints did not differ from the intact I group to control C group and treatment (ES and GT + ES) groups when assessed 30 days after SCI (**Figure 2**). The knee joint movements were significantly impaired in the C and ES groups ($P < 0.05$) whereas those in the GT + ES group appeared to be recovered nearly to the level of intact rats (I group). The mean area of tibialis anterior muscle fibers was significantly decreased in the C and ES groups compared with I group ($P < 0.05$). Importantly, the mean area of muscle fibers in the GT + ES group was significantly higher than that in C and ES groups and it did not differ from that in the I group ($P < 0.05$; **Figure 3**).

Electrophysiological evaluation of gastrocnemius muscle

In response to electrical stimulations at the sciatic nerve, M-response and H-reflex were recorded at the medial head of gastrocnemius muscle of each hindlimb. M-response in SCI animals (SCI group) showed polyphasic waves (**Figure 4**). Thresholds and latencies of both M-response and H-reflex did not show any significant differences across experimental groups. Although amplitudes of M-responses in all SCI animals were slightly decreased compared to intact animals, there was no significant difference in maximal M-response across groups which implied no decreased muscle tones of gastrocnemius muscles after SCI. These results are consistent with the data on gastrocnemius muscle fiber area, which did not differ in all experimental groups from those in the I group (**Figure 3**). To compare the size of H-reflex between animals across different groups, amplitudes of H-reflex were normalized with the maximal size of M-responses. We found increased H/M ratios i.e., enhanced monosynaptic responses of spinal motoneurons in the GT + ES group when compared with intact animals in the I group ($P < 0.05$; **Figure 4**).

Post-traumatic spinal cord remodeling

Morphometric analysis of gray and white matter sparing

The severity of SCI measured at the 30th day after SCI was consistent with the findings from our previous study (Izmailov et al., 2017a). Morphometric analysis of spinal cord segments caudal to the injury epicenter showed significantly different sparing of the gray matter across experimental groups. The volume of the preserved tissue in the caudal segments was significantly higher in the GT + ES group than that in the ES and C groups ($P < 0.05$; **Figure 5B**). This supports that the combination treatment but not EES alone improved sparing of the gray matter after SCI.

It is known that axonal growth through the epicenter of injured mammalian spinal cord is extremely limited. In the current study, axonal regeneration in the white matter was evaluated by counting the number of myelinated axons in ventral, lateral and dorsal funiculi on both sides of the spinal cord at the epicenter and 5 mm away from to the site of injury. No significant changes were found in all three funiculi at both spinal segments. There was a tendency of increase in myelinated axon numbers in the caudal segment (5 mm distal from the epicenter of injury) in all experimental groups (**Figure 6**). In rats from ES and GT + ES groups, the tendency of increased myelinated axon numbers was more noticeable which may suggest a beneficial effect of EES on the sparing of myelinated fibers in the white matter.

Immunofluorescence analysis of the spinal cord

Stress and apoptosis markers

At 30 days post-SCI, the level of a stress protein, Hps27, was significantly higher in the ventral horn of the spinal cord in animals from the ES and GT + ES groups than that in the control (C) group ($P < 0.05$; **Figure 7A** and **B**). Immunoexpression of Hps27 did not differ between the ES and GT + ES groups. Hps27 was significantly up-regulated in the GT + ES group than in the intact I group ($P < 0.05$; **Figure 7B**).

Caspase 3-positive, apoptotic cells were found in ventral (VH, 5.27 ± 3.13) and dorsal (DREZ, 8.53 ± 4.65) horns of the C group but not in all investigated regions (VH, DREZ, CC, CST, VF, LF and DF) of the ES and GT + ES groups (**Figure 7C**). Thus, EES increased the expression levels of Hps27 and reduced

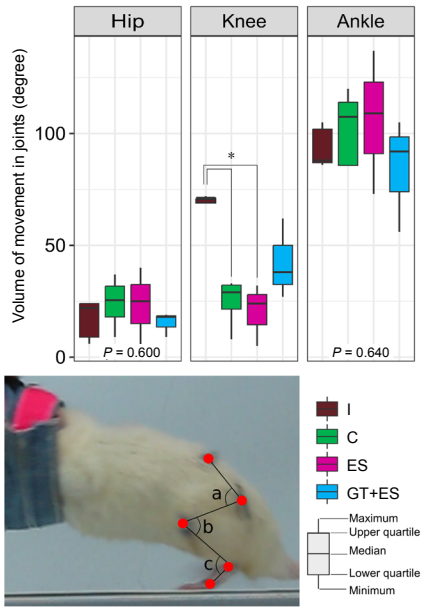

Figure 2 | Locomotor activity of hindlimbs 30 days after spinal cord injury (SCI).

Volume of movement in hip (a), knee (b) and ankle (c) joints was estimated by measuring the angles in degrees. Data are visualized using box plots, and expressed as median (interquartile range), *$P < 0.05$ (Dunn's test). I group: Intact rats ($n = 6$); C group: control SCI rats without treatment ($n = 6$); ES group: SCI rats subjected to epidural electrical stimulation alone ($n = 4$); GT + ES group: SCI rats subjected to electrical stimulation combined with gene therapy ($n = 5$).

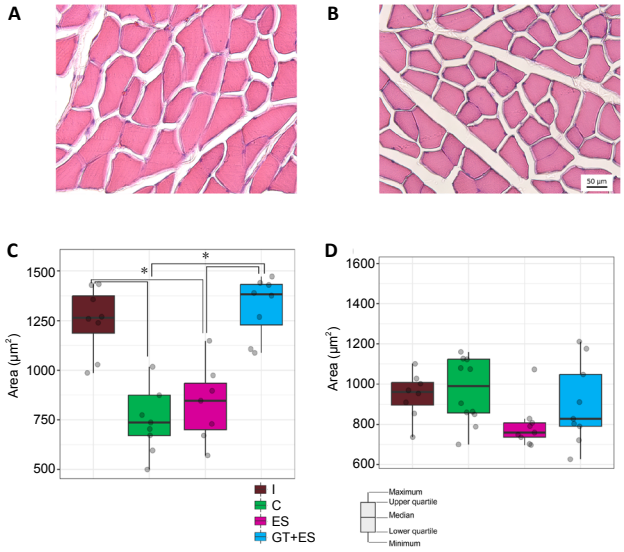

Figure 3 | Evaluation of muscle fiber area in the hindlimb skeletal muscles 30 days after spinal cord injury (SCI).

Frozen cross sections of tibialis anterior muscle (A) and medial head of gastrocnemius muscle (B) were stained with hematoxylin and eosin and the mean area of the skeletal muscle fibers was measured. The mean area of the tibialis anterior muscle (C) and gastrocnemius muscle (D) fibers was compared between groups. Data are visualized using box plots and expressed as median (interquartile range), *$P < 0.05$ (Dunn's test). I group: Intact rats ($n = 6$); C group: control SCI rats without treatment ($n = 6$); ES group: SCI rats subjected to epidural electrical stimulation alone ($n = 4$); GT + ES group: SCI rats subjected to electrical stimulation combined with gene therapy ($n = 5$).

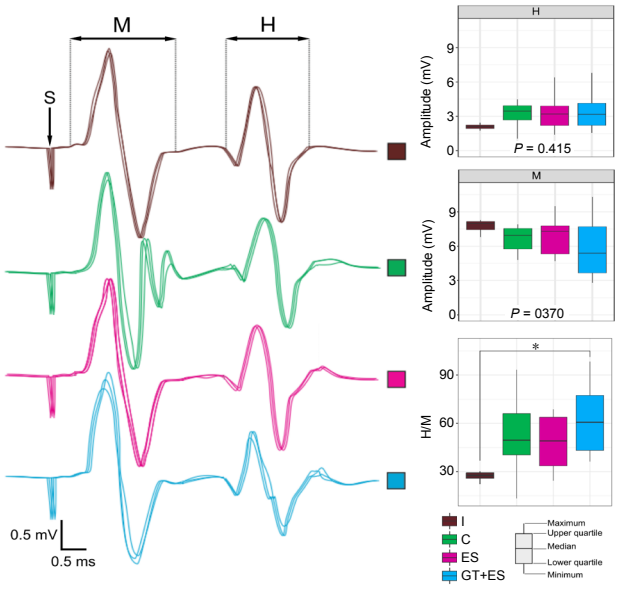

Figure 4 | Electrophysiological investigation of the gastrocnemius muscle 30 days after spinal cord injury (SCI).
M-response of the muscle in control (C; SCI only) group demonstrates several phases (polyphasic M-response). The ratio of maximal sizes of H- and M-responses (H/M ratio) % = [H_{max}/M_{max}] × 100. Data are visualized using box plots and expressed as median (interquartile range), *P < 0.05 (Dunn's test). I group: Intact rats (n = 6); C group: control SCI rats without treatment (n = 6); ES group: SCI rats subjected to epidural electrical stimulation alone (n = 4); GT + ES group: SCI rats subjected to electrical stimulation combined with gene therapy (n = 5).

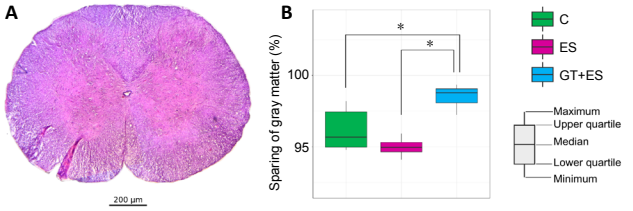

Figure 5 | Sparing of spinal cord gray matter 30 days after spinal cord injury (SCI).
(A) Cross section of a caudal segment of the spinal cord stained with hematoxylin and eosin from the GT + ES group. Volume of the cysts and total area of gray matter were measured and converted into the percent data. (B) Comparative analysis of the gray matter preservation in experimental groups. Data are visualized using box plots, and expressed as median (interquartile range), *P < 0.05 (Dunn's test). C group: Control SCI rats without treatment (n = 6); ES group: SCI rats subjected to epidural electrical stimulation alone (n = 4); GT + ES group: SCI rats subjected to electrical stimulation combined with gene therapy (n = 5).

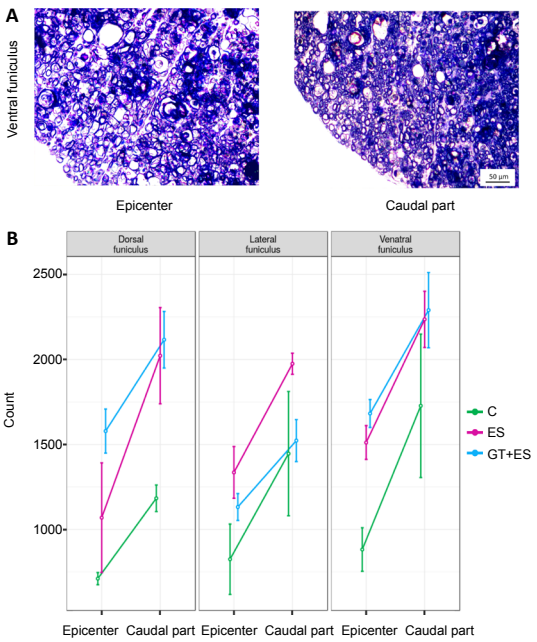

Figure 6 | Sparing of spinal cord white matter 30 days after spinal cord injury (SCI).
The average numbers of the myelinated fibers were counted in the ventral, lateral, and dorsal columns at the site of contusion injury and 5 mm caudal to the lesion epicenter. (A) Semi-thin transverse sections of the spinal cords from epicenter and caudal part stained with methylene blue dye. Presented is a white matter (ventral funiculus) of a rat from the GT + ES group. (B) Comparative analysis of the white matter preservation in the experimental groups. Data are expressed as mean ± SEM. C group: Control SCI rats without treatment (n = 6); ES group: SCI rats subjected to epidural electrical stimulation alone (n = 4); GT + ES group: SCI rats subjected to electrical stimulation combined with gene therapy (n = 5).

apoptosis in caudal segments of the injured spinal cord, at least, at 30 days after injury.

Synaptic protein markers
The analysis of presynaptic (synaptophysin) and postsynaptic (PSD95) proteins in the ventral horns of the spinal cord showed differences across the experimental groups (**Figure 8**). The level of synaptophysin was decreased in all rats with SCI compared with I group (P < 0.05). However, the immunoexpression of synaptophysin was significantly higher in the GT + ES group compared to ES and C groups (P < 0.05) which did not differ from each other.

The mean fluorescence intensity of the PSD95 in the I group was significantly higher compared with the C, ES, and GT + ES groups (P < 0.05). The level of PSD95 in the GT + ES group was significantly higher compared with C and ES groups (P < 0.05), both of which did not differ from each other (**Figure 8**). These results suggest the beneficial effects of the *ex vivo* triple gene therapy on the recovery of synaptic molecule expression in the ventral horn.

UCBMC performance *in vitro* and *in vivo* study

Production of recombinant VEGF, GDNF and NCAM by gene modified UCBMCs in vitro

The levels of soluble recombinant human molecules VEGF, GDNF, and NCAM were analyzed in the conditioned culture media after incubation of gene modified UCBMCs by ELISA assay. The levels of the VEGF, GDNF, and NCAM were increased 68-, 15- and 242-fold in supernatants of UCBMCs + Ad5-*VEGF*/*GDNF*/*NCAM* when compared with naïve UCBMC (**Figure 9**). This implies that gene engineered UCBMCs may efficiently synthesize and secrete recombinant therapeutic molecules *in vivo*.

Homing and viability of the UCBMCs in rat spinal cord

Anti-human nuclear antigen (HNA) antibodies were used to demonstrate homing and survival of human UCBMCs in rostral segment of spinal cord of rats from GT + ES group (**Figure 10**). On the 30th day after intrathecal infusion of UCBMCs, HNA-positive cells were found in gray and white matter of spinal cord tissue. The round shaped cells approximately 8–10 µm in diameter had a large nucleus surrounded by a thin rim of cytoplasm. The fact that HNA-positive cells were observed in the rostral segments provided the evidence that intrathecally infused UCBMCs by cerebrospinal fluid might have passed the epicenter of injury and disseminated throughout the central nervous system. It is worth to mention that HNA-positive cells maintained their viability for 30 days after transplantation.

In vivo immunofluorescence staining study of recombinant gene expression in UCBMCs

Microscopic studies showed HNA-positive cells producing recombinant molecules (VEGF, GDNF, and NCAM) in both

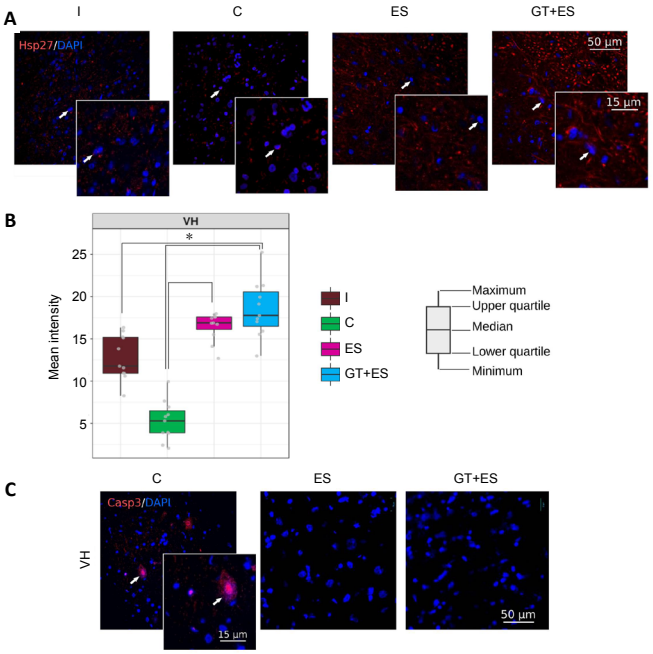

Figure 7 | **Immunoexpression of Hsp27 and Caspase 3 in spinal cord 30 days after spinal cord injury (SCI).**
(A) Immunofluorescence staining with antibodies against Hsp27 (red). Arrows indicate nuclei. (B) Fluorescence density value of Hsp27 immunoreactivity. Data are visualized using box plots and expressed as median (interquartile range), *P < 0.05 (Dunn's test). (C) Immunofluorescence staining with antibodies against Caspase 3 (red). Arrows indicate the apoptotic cells. Nuclei (blue) were counterstained with 4′,6-diamidino-2-phenylindole (DAPI). I group: Intact rats (n = 6); C group: control SCI rats without treatment (n = 6); ES group: SCI rats subjected to epidural electrical stimulation alone (n = 4); GT + ES group: SCI rats subjected to electrical stimulation combined with gene therapy (n = 5).

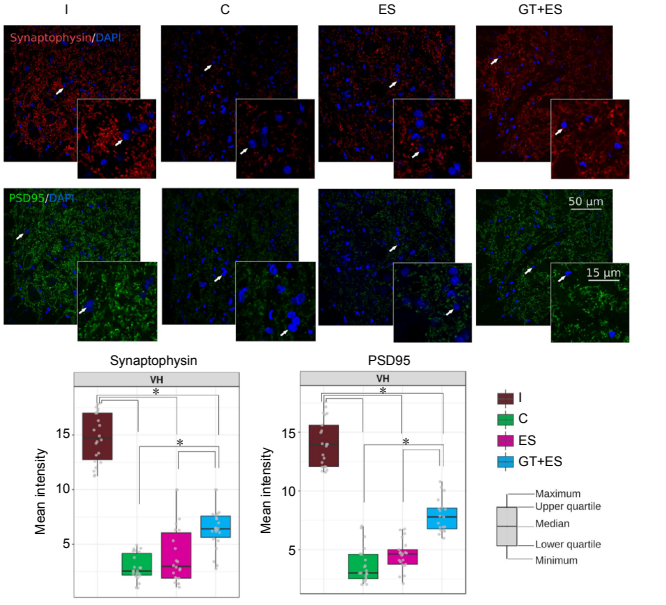

Figure 8 | **Immunoexpression of synaptic proteins synaptophysin and PSD95 in spinal cord ventral horns (VH) 30 days after spinal cord injury (SCI).**
Upper panel: Immunofluorescence staining with antibodies against synaptophysin (red) and PSD95 (green). Nuclei (blue) were counterstained with 4′,6-diamidino-2-phenylindole (DAPI). Lower panel: Fluorescence density value of synaptophysin and PSD95. Arrows indicate nuclei. Data are visualized using box plots and expressed as median (interquartile range), *P < 0.05 (Dunn's test). I group: Intact rats (n = 6); C group: control SCI rats without treatment (n = 6); ES group: SCI rats subjected to epidural electrical stimulation alone (n = 4); GT + ES group: SCI rats subjected to electrical stimulation combined with gene therapy (n = 5).

gray and white matters of the spinal cord (**Figure 10**). These data indicate that UCBMCs injected below the injury epicenter (L4–5 levels) migrated to the rostral segment and produced therapeutic molecules within 30 days after xenotransplantation.

Discussion

In the present study, we evaluated a potential combinatorial strategy with the clinically relevant EES and cell-mediated delivery of therapeutic genes that have shown beneficial effects in our previous SCI model (Islamov et al., 2017; Izmailov et al., 2017a). For gene therapy, the rats were intrathecally infused 4 hours after SCI with genetically modified UCBMCs that simultaneously express three therapeutic genes encoding *VEGF165*, *GDNF* and *NCAM1*. UCBMCs have been shown to secrete neurotrophic factors, such as GDNF, VEGF, brain-derived neurotrophic factor, nerve growth factor, neurotrophin-3, and NT-5 in experiments *in vitro* (Fan et al., 2005; Pimentel-Coelho et al., 2012). In blood, expression of NCAM (CD56) is associated with natural killer cells, monocytes, and T-cells (Van Acker et al., 2017) and has a membrane-associated isoform and a soluble isoform (Krog et al., 1992). Previously, we showed the important role of the recombinant NCAM production in UCB-MCs for their survival in host spinal cord (Safiullov et al., 2015). Thus, gene encoding *NCAM* in UCBMCs was used to improve migration potential and increase viability of the transplanted UCBMCs in the host spinal cord.

EES was given both above the injury epicenter to improve the survivability of the preserved neurons and their myelinated axons and below the level of injury to activate local neural circuits deprived of connections with the supraspinal neurons. The combined EES and gene therapy showed limited but significant advantages over EES alone 30 days post-SCI.

The implantation of 12-channel headplugs fixed on the animal skull restricted our possibility in using standard BBB test for evaluation of functional recovery. Although we have implanted headplugs before SCI surgery and no animals with implants showed abnormal locomotion, the head implant may distract them from the testing or affect the recovery of rats' locomotion over the time course after SCI. In addition, a small number of animals in this proof of concept study would make the interpretation of results from complex locomotor behavioral testing like BBB even harder. For these reasons, we performed relatively subjective joint kinematic evaluations once on the final, 30th day post-operation. Moreover, it was shown that this kinematic assessment was in line with BBB test results (Hansen et al., 2012).

Evaluation of joint kinematics is one of the effective methods for analyzing the functional recovery of the conduction pathways of the spinal cord after contusion injury. Tibialis anterior (ankle flexor), gastrocnemius (ankle extensor), gluteus medius (hip extensor/abductor), sartorius (hip flexor/knee extensor), and semitendinosus (knee flexor/hip extensor) are involved in well-established hindlimb kinematics (Watson et al., 2009). After SCI, semitendinosus muscle unlike the other hindlimb skeletal muscles remains impaired for a longer period and EMG activity of semitendinosus muscle may serve as a marker of incomplete recovery (Hansen et al., 2012). The current data showed that only the group with combined EES and genetic treatments improved the recovery of the knee joint kinematics but not in the group with EES alone confirming the beneficial effect of *ex vivo* triple gene therapy on the recovery of hindlimb locomotor activity as it was shown previously (Izmailov et al., 2017b).

An interesting finding was the correlation between the knee joint kinematics and the preservation of corresponding hindlimb muscles. At 30 days after SCI, the GT + ES group showed the improved knee joint performance, which was consistent with the data on preservation of muscle fiber area

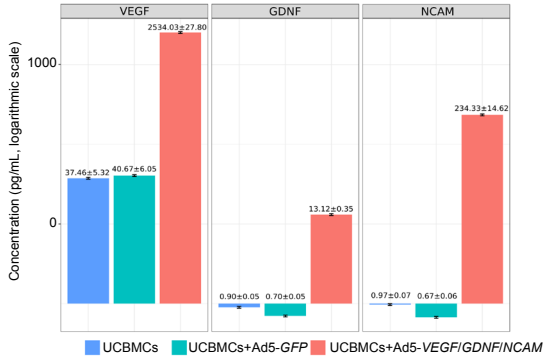

Figure 9 | Recombinant GDNF, VEGF, and NCAM produced by gene-modified UCBMCs *in vitro*.
Enzyme-linked immunosorbent assay was used to analyze soluble human VEGF, GDNF, and NCAM in the conditioned culture media. The level of recombinant molecules was estimated in supernatant 72 hours after incubation of naïve UCBMCs, UCBMCs transduced with Ad5 carrying gene encoding reporter green fluorescent protein (UCBMCs + Ad5-GFP) and UCBMCs simultaneously transduced with Ad5-*VEGF*, Ad5-*GDNF*, and Ad5-*NCAM* (UCBMCs + Ad5-*VEGF*/*GDNF*/*NCAM*). Data are presented as the mean ± SEM. GDNF: Glial cell-line derived neurotrophic factor; GFP: green fluorescent protein; NCAM: neural cell adhesion molecule; UCBMCs: umbilical cord blood mononuclear cells; VEGF: vascular endothelial growth factor.

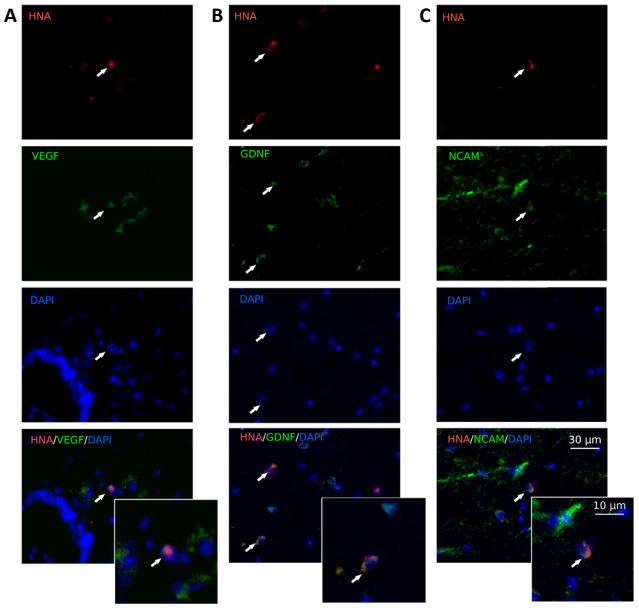

Figure 10 | Immunoexpression of recombinant GDNF, VEGF, and NCAM in gene-modified UCBMCs *in vivo*.
Double immunofluorescence staining of UCBMCs in injured spinal cord 30 days after intrathecal infusion. Anti-HNA antibodies were used for identification of UCBMCs. Human recombinant molecules were identified with antibodies against human specific VEGF, GDNF, and NCAM. (A) HNA-positive cells (red) expressing VEGF (green). (B) HNA-positive cells (red) expressing GDNF (green). (C) HNA-positive cells (red) expressing NCAM (green). Nuclei (blue) were counterstained with DAPI. Arrows indicate UCBMCs. DAPI: 4′,6-Diamidino-2-phenylindole; GDNF: glial cell-line derived neurotrophic factor; HNA: human nuclear antigen; NCAM: neural cell adhesion molecule; UCBMCs: umbilical cord blood mononuclear cells; VEGF: vascular endothelial growth factor.

in tibialis anterior, an ankle flexor. These data may also be in line with results on histological evaluation of the spinal cord in GT + ES group at the L2–4 level. The higher preservation of the gray matter and higher expression levels of synaptic proteins (PSD95 and synaptophysin) in the ventral horn suggested that EES in combination with cell-mediated triple gene therapy have the positive synergistic effect on the preservation of motoneurons, which may prevent the atrophy of tibialis anterior muscle contributing to the better recovery of the knee joint following SCI.

The EMG analysis of the H-reflex is a commonly used clinical tool in neurological testing (Misiaszek, 2003). The alterations in the M-wave and H-reflex are highly correlated with the motor unit activities (McNeil et al., 2013). The amplitude of M-wave evoked by direct electrical stimulations to motor nerves represents the muscle tone while the amplitude of H-reflex reflects the excitability of monosynaptic connections between Ia muscle afferents and spinal motoneurons (Tucker et al., 2005). The amplitude of M-wave or H-reflex recorded from the gastrocnemius muscle did not show any significant differences between intact and all experimental groups. Morphometric evaluation of the corresponding muscle fibers in gastrocnemius muscle (ankle extensor) also showed no differences in all examined groups. These demonstrate that preservation of gastrocnemius muscle fibers, at least, for 30 days after SCI was associated with no changes in muscle tone (M-wave or H-reflex) and the ankle joint kinematics in all studied groups. This also suggests that the hip joint kinematics may have been preserved for 30 days in all groups with SCI.

Normalized H/M ratio is often used to measure the extent of central modulation on spinal motoneurons. After SCI, H/M ratio remarkably increased even in incomplete injury (Lee et al., 2005, 2009) which may be mainly due to loss of inhibitory supraspinal controls. It has been found that decreased expression of potassium-chloride cotransporter (KCC2) disrupted chloride equilibrium in spinal motoneurons below the level of injury contributing to the increased H-reflex and the development of spasticity after SCI (Boulenguez et al., 2010). However, enhanced H-reflex may be required for modulation of spared local motor units below the level of injury as the persistent or even progressed increase of H-reflex was observed while the locomotor function improved over time after incomplete SCI (Lee et al., 2005, 2009). In this study, we found an increase of H/M ratio in rats with combined therapy. As the general behavior evaluation demonstrated less spastic movement in animals with combined therapy, the elevated H-reflex appeared to be a sign of increased motoneuron excitability in lumbar spinal motoneurons that may be related to the better kinematics of the knee joint seen in those animals. The other reason of the elevated H/M ratio may be due to remodeling of the synapsis on the survived neurons as shown by the enhanced expression of synaptic proteins (synaptophysin and PSD95) in rats subjected to combined EES and gene therapy.

It was surprising that the epidural stimulation alone was not sufficient to improve hindlimb joint kinematics, H/M ratios, or general behaviors. It appears somewhat controversial to the previous reports that demonstrated beneficial functional outcomes after epidural stimulations (Barbeau and Rossignol, 1991; Iwahara et al., 1991; Dimitrijevic et al., 1998; Gerasimenko et al., 2003). Up to date, there are no established methods of EES for preclinical SCI models or no standard clinical protocol yet. The most commonly used EES protocol has stimulated lumbosacral spinal circuitry to regenerate locomotor stepping abilities which has been demonstrated in both spinalized animals and in patients with complete SCI (Gill et al., 2018). The current study used a multisite protocol of EES at L2 level to improve stepping behavior in hindlimbs and at C5 level to promote axonal regeneration through the epicenter of injury. However, our epidural stimulation protocol applied in this study sufficed to generate the neuroprotective effects as discussed below but not to reestablish nerve function after SCI. One of the possible explanations is that the recovery of hindlimb behavior requires longer than 30 days after SCI. We chose 30 days based on our previous *ex vivo* gene delivery that improved locomotor function compared to control SCI rats (Mukhamedshina et al., 2016; Izmailov et al., 2017a). Although a further investigation is required, it seems that expression of recombinant VEGF, GDNF and NCAM may require for better hindlimb function recovery, at least, for the

first 30 days after SCI. It is worth to mention that EES cannot be started in the period of spinal shock which may last several days after SCI (Gill et al., 2018) whereas the gene therapy could be applied in the acute phase of SCI (Izmailov et al., 2017a). These need to be considered in the future study to find an optimal protocol of EES combined with the beneficial gene therapy.

The spinal cord cytoarchitecture dramatically changes after injury. Death of neurons, glial cells, and their precursors and disruption of descending and ascending spinal tracts lead to cavitation, demyelination, and astrogliosis (Thuret et al., 2006). Our data demonstrated that when compared to untreated rats (C group), the rats receiving epidural stimulations in the ES and GT + ES groups had increased expression of Hsp27 (neuroprotection) but reduced expression of Caspase3 (apoptosis), suggesting that epidural stimulations were neuroprotective. Indeed, those animals in the ES and GT + ES group showed better preservation of myelinated axons in the white matter, which has been previously shown as one of neuroprotective effects of the epidural stimulation (Kakinohana et al., 2005). Combined EES and gene therapy improved sparing of the gray matter in lumbar segments caudal to the injury epicenter resulting in better functional recovery e.g., improved knee joint kinematics and enhanced spinal motoneuron excitability post-SCI. These data are consistent with our previous research (Izmailov et al., 2017a) that reduction of the ongoing apoptosis and preservation of the gray matter were associated with better functional outcome in rats with SCI subjected to *ex vivo* gene treatment.

Collectively, we have found improved functional outcomes in rats from the GT + ES group in terms of hindlimb kinematics and enhanced H-reflex which were supported by the better results on the decreased ongoing apoptosis and the sparing of the gray and white matter in the injured spinal cord in those animals. Despite of incomplete effects of EES alone at 30 days after SCI, it should be noted that the features of post-traumatic spinal cord remodeling after *ex vivo* gene therapy has been consistent with our previous results (Izmailov et al., 2017a). Thus, the results of this study demonstrated the potent that *ex vivo* triple gene therapy combined with clinically established electrical stimulation therapy may maximize the beneficial effects of each treatment on morpho-functional recovery of spinal cord after severe contusion in rats.

A translational research will be necessary to optimize the EES protocol in SCI patients undergoing gene therapy. To obtain reliable effects of electrical stimulations and comprehensively understand cellular and molecular changes, we used EES, an invasive method, in SCI rats subjected to *ex vivo* triple gene therapy. There might be several considerations to overcome the limitations of the current proof of concept study. First, non-invasive methods like electro-magnetic or transcutaneous stimulations can be used. A preclinical study combined the electro-magnetic stimulation with *in vivo* gene therapy for treatment of T10 contusion SCI in rat models (Petrosyan et al., 2015). These authors intraspinally injected adeno-associated virus serotype 10 expressing neurotrophin-3 around the injury epicenter. After 5 weeks of electro-magnetic stimulations above the injury at T2 level, those injured, genetically treated rats showed better outcomes in synaptic transmission, anatomical plasticity, and recovery of locomotor function. As transcutaneous electrical stimulations have been well studied in humans (Sayenko et al., 2015), the potential use of non-invasive stimulations would be achievable. Second, a clinically adequate experimental animal model can be used in a preclinical study to better reproduce the clinical consequences of acute and chronic SCI as in humans. In this regard, studies on the SCI model in large animals like pigs are quite promising (Swindle et al., 2012). Lastly, the beneficial effects of EES and gene therapy would need to be confirmed in male rats. As mentioned in the method, due to the ease and consistency of bladder management after SCI, only female rats were used in this study. This will be especially critical considering the fact that SCI is usually predominant in young males (Hamid et al., 2018).

Conclusion

Despite numerous previous animal experiments and clinical trials, there is no established treatment protocol for SCI in practical medicine. In the present study, we proposed a potential strategy of epidural electrical stimulation combined with *ex vivo* triple gene therapy for SCI treatment. Intrathecal infusion of genetically engineered UCBMCs producing recombinant therapeutic molecules (VEGF, GDNF, and NCAM) combined with multisite electrotherapy demonstrated beneficial effects on post-traumatic recovery of the spinal cord.

Author contributions: *Writing the manuscript: RRI and HJL; modeling of spinal cord injury: FOF and VAM; behavioral testing: FVB and MSK; electrophysiological investigation; MES and AAE; in vitro study of gene-modified umbilical cord blood mononuclear cells: IIS and AAR; histological investigation: AAI and TVP; approval of final version of this paper: all authors.*
Conflicts of interest: *The authors declare no conflicts of interest.*
Financial support: *This study was supported by the grant of Russian Science Foundation, No. 16-15-00010 (to RRI). AAR was supported by the Russian Government Program of Competitive Growth of Kazan Federal University.*
Institutional review board statement: *Animal experiments were approved by the Kazan State Medical University Animal Care and Use Committee (approval No. 2.20.02.18) on February 20, 2018.*
Copyright license agreement: *The Copyright License Agreement has been signed by all authors before publication.*
Data sharing statement: *Datasets analyzed during the current study are available from the corresponding author on reasonable request.*
Plagiarism check: *Checked twice by iThenticate.*
Peer review: *Externally peer reviewed.*

References

Barbeau H, Rossignol S (1991) Initiation and modulation of the locomotor pattern in the adult chronic spinal cat by noradrenergic, serotonergic and dopaminergic drugs. Brain Res 546:250-260

Boulenguez P, Liabeuf S, Bos R, Bras H, Jean-Xavier C, Brocard C, Stil A, Darbon P, Cattaert D, Delpire E, Marsala M, Vinay L (2010) Down-regulation of the potassium-chloride cotransporter KCC2 contributes to spasticity after spinal cord injury. Nat Med 16:302-307.

Clapham DE (2007) Calcium signaling. Cell 131:1047-1058.

Courtine G, Song B, Roy RR, Zhong H, Herrmann JE, Ao Y, Qi J, Edgerton VR, Sofroniew M V (2008) Recovery of supraspinal control of stepping via indirect propriospinal relay connections after spinal cord. Nat Med 14:69-74.

Dimitrijevic MR, Gerasimenko Y, Pinter MM (1998) Evidence for a spinal central pattern generator in humans. Ann N Y Acad Sci 860:360-376.

Gerasimenko Y, Gorodnichev R, Puhov A, Moshonkina T, Savochin A, Selionov V, Roy RR, Lu DC, Edgerton VR (2015) Initiation and modulation of locomotor circuitry output with multisite transcutaneous electrical stimulation of the spinal cord in noninjured humans. J Neurophysiol 113:834-842.

Gerasimenko YP, Avelev VD, Nikitin OA, Lavrov IA (2003) Initiation of locomotor activity in spinal cats by epidural stimulation of the spinal cord. Neurosci Behav Physiol 33:247-254.

Gerfen CR, Paxinos G (2004) The rat nervous system. San Diego: Academic Press.

Gill ML, Grahn PJ, Calvert JS, Linde MB, Lavrov IA, Strommen JA, Beck LA, Sayenko DG, Van Straaten MG, Drubach DI, Veith DD, Thoreson AR, Lopez C, Gerasimenko YP, Edgerton VR, Lee KH, Zhao KD (2018) Neuromodulation of lumbosacral spinal networks enables independent stepping after complete paraplegia. Nat Med 24:1677-1682.

Hamid R, Averbeck MA, Chiang H, Garcia A, Al Mousa RT, Oh SJ, Patel A, Plata M, Del Popolo G (2018) Epidemiology and pathophysiology of neurogenic bladder after spinal cord injury. World J Urol 36:1517-1527.

Hamid S, Hayek R (2008) Role of electrical stimulation for rehabilitation and regeneration after spinal cord injury: an overview. Eur Spine J 17:1256-1269.

Hansen CN, Linklater W, Santiago R, Fisher LC, Moran S, Buford JA, Michele Basso D (2012) Characterization of recovered walking patterns and motor control after contusive spinal cord injury in rats. Brain Behav 2:541-552.
Harvie DS, Smith RT, Hunter EV, Davis MG, Sterling M, Moseley GL (2017) Using visuo-kinetic virtual reality to induce illusory spinal movement: the MoOVi Illusion. PeerJ 5:e3023.
Ho CH, Triolo RJ, Elias AL, Kilgore KL, DiMarco AF, Bogie K, Vette AH, Audu ML, Kobetic R, Chang SR, Chan KM, Dukelow S, Bourbeau DJ, Brose SW, Gustafson KJ, Kiss ZH, Mushahwar VK (2014) Functional electrical stimulation and spinal cord injury. Phys Med Rehabil Clin N Am 25:631-654.
Ichim TE, Solano F, Lara F, Paris E, Ugalde F, Rodriguez JP, Minev B, Bogin V, Ramos F, Woods EJ, Murphy MP, Patel AN, Harman RJ, Riordan NH (2010) Feasibility of combination allogeneic stem cell therapy for spinal cord injury: a case report. Int Arch Med 3:30.
Ichiyama RM, Gerasimenko Y, Jindrich DL, Zhong H, Roy RR, Edgerton VR (2008) Dose dependence of the 5-HT agonist quipazine in facilitating spinal stepping in the rat with epidural stimulation. Neurosci Lett 438:281-285.
Ichiyama RM, Gerasimenko YP, Zhong H, Roy RR, Edgerton VR (2005) Hindlimb stepping movements in complete spinal rats induced by epidural spinal cord stimulation. Neurosci Lett 383:339-344.
Islamov RR, Rizvanov AA, Mukhamedyarov MA, Salafutdinov II, Garanina EE, Fedotova VY, Solovyeva VV, Mukhamedshina YO, Safiullov ZZ, Izmailov AA, Guseva DS, Zefirov AL, Kiyasov AP, Palotas A (2015) Symptomatic improvement, increased life-span and sustained cell homing in amyotrophic lateral sclerosis after transplantation of human umbilical cord blood cells genetically modified with adeno-viral vectors expressing a neuro-protective factor and a neur. Curr Gene Ther 15:266-276.
Islamov RR, Sokolov ME, Bashirov FV, Fadeev FO, Shmarov MM, Naroditskiy BS, Povysheva TV, Shaymardanova GF, Yakupov RA, Chelyshev YA, Aleksandrovich LI (2017) A pilot study of cell-mediated gene therapy for spinal cord injury in mini pigs. Neurosci Lett 644:67-75.
Iwahara T, Atsuta Y, Garcia-Rill E, Skinner RD (1991) Locomotion induced by spinal cord stimulation in the neonate rat in vitro. Somatosens Mot Res 8:281-287.
Izmailov AA, Povysheva TV, Bashirov FV, Sokolov ME, Fadeev FO, Garifulin RR, Naroditsky BS, Logunov DY, Salafutdinov II, Chelyshev YA, Islamov RR, Lavrov IA (2017a) Spinal cord molecular and cellular changes induced by adenoviral vector- and cell-mediated triple gene therapy after severe contusion. Front Pharmacol 8:813.
Izmailov AA, Sokolov ME, Bashirov FV, Fadeev FO, Markosyan VA, Garifulin RR, Lisyukov AN, Kuznetsov MS, Islamov RR (2017b) Comparative analysis of efficiency of direct and cell-mediated gene therapy of rats with contusion spinal cord injury. Genes Cells 12:53-59.
Kakinohana M, Harada H, Mishima Y, Kano T, Sugahara K (2005) Neuroprotective effect of epidural electrical stimulation against ischemic spinal cord injury in rats: electrical preconditioning. Anesthesiology 103:84-92.
Lavrov I, Dy CJ, Fong AJ, Gerasimenko Y, Courtine G, Zhong H, Roy RR, Edgerton VR (2008) Epidural stimulation induced modulation of spinal locomotor networks in adult spinal rats. J Neurosci 28:6022-6029.
Lavrov I, Gerasimenko YP, Ichiyama RM, Courtine G, Zhong H, Roy RR, Edgerton VR (2006) Plasticity of spinal cord reflexes after a complete transection in adult rats: relationship to stepping ability. J Neurophysiol 96:1699-1710.
Lebedev SV, Timofeyev SV, Zharkov AV, Schipilov VG, Chelyshev JA, Masgutova GA, Chekhonin VP (2008) Exercise tests and BBB method for evaluation of motor disorders in rats after contusion spinal injury. Bull Exp Biol Med 146:489-494.
Lee HJ, Jakovcevski I, Radonjic N, Hoelters L, Schachner M, Irintchev A (2009) Better functional outcome of compression spinal cord injury in mice is associated with enhanced H-reflex responses. Exp Neurol 216:365-374.
Lee JK, Emch GS, Johnson CS, Wrathall JR (2005) Effect of spinal cord injury severity on alterations of the H-reflex. Exp Neurol 196:430-440.
Leinninger GM, Backus C, Uhler MD, Lentz SI, Feldman EL (2004) Phosphatidylinositol 3-kinase and Akt effectors mediate insulin-like growth factor-I neuroprotection in dorsal root ganglia neurons. FASEB J 18:1544-1546.
Lilienbaum A, Israël A (2003) From calcium to NF-kappa B signaling pathways in neurons. Mol Cell Biol 23:2680-2698.
Lim ST, Airavaara M, Harvey BK (2010) Viral vectors for neurotrophic factor delivery: a gene therapy approach for neurodegenerative diseases of the CNS. Pharmacol Res 61:14-26.
Liu J, Han D, Wang Z, Xue M, Zhu L, Yan H, Zheng X, Guo Z, Wang H (2013) Clinical analysis of the treatment of spinal cord injury with umbilical cord mesenchymal stem cells. Cytotherapy 15:185-191.
Martin R, Sadowsky C, Obst K, Meyer B, McDonald J (2012) Functional electrical stimulation in spinal cord injury: from theory to practice. Top Spinal Cord Inj Rehabil 18:28-33.
McNeil CJ, Butler JE, Taylor JL, Gandevia SC (2013) Testing the excitability of human motoneurones. Front Hum Neurosci 7:1-9.
Misiaszek JE (2003) The H-reflex as a tool in neurophysiology: Its limitations and uses in understanding nervous system function. Muscle Nerve 28:144-160.
Mittereder N, March KL, Trapnell BC (1996) Evaluation of the concentration and bioactivity of adenovirus vectors for gene therapy. J Virol 70:7498-7509.
Mukhamedshina YO, Shaymardanova GF, Garanina EE, Salafutdinov II, Rizvanov AA, Islamov RR, Chelyshev YA, Rizvanov AA, Islamov RR, Chelyshev YA, Rizvanov AA, Islamov RR, Chelyshev YA (2016) Adenoviral vector carrying glial cell-derived neurotrophic factor for direct gene therapy in comparison with human umbilical cord blood cell-mediated therapy of spinal cord injury in rat. Spinal Cord 54:347-359.
Peng HH, Wu S, Davis JJ, Wang L, Roth JA, Marini 3rd FC, Fang B (2006) A rapid and efficient method for purification of recombinant adenovirus with arginine-glycine-aspartic acid-modified fibers. Anal Biochem 354:140-147.
Petrosyan HA, Alessi V, Hunanyan AS, Sisto SA, Arvanian VL (2015) Spinal electromagnetic stimulation combined with transgene delivery of neurotrophin NT-3 and exercise: novel combination therapy for spinal contusion injury. J Neurophysiol 114:2923-2940.
Rafii MS, Baumann TL, Bakay RAE, Ostrove JM, Siffert J, Fleisher AS, Herzog CD, Barba D, Pay M, Salmon DP, Chu Y, Kordower JH, Bishop K, Keator D, Potkin S, Bartus RT (2014) A phase1 study of stereotactic gene delivery of AAV2-NGF for Alzheimer's disease. Alzheimers Dement 10:571-581.
Sayenko DG, Atkinson DA, Dy CJ, Gurley KM, Smith VL, Angeli C, Harkema SJ, Edgerton VR, Gerasimenko YP (2015) Spinal segment-specific transcutaneous stimulation differentially shapes activation pattern among motor pools in humans. J Appl Physiol 118:1364-1374.
Shah PK, Lavrov I (2017) Spinal epidural stimulation strategies: clinical implications of locomotor studies in spinal rats. Neuroscientist 23:664-680.
Swindle MM, Makin A, Herron AJ, Clubb FJ, Frazier KS (2012) Swine as models in biomedical research and toxicology testing. Vet Pathol 49:344-356.
Taccola G, Sayenko D, Gad P, Gerasimenko Y, Edgerton VR (2018) And yet it moves: Recovery of volitional control after spinal cord injury. Prog Neurobiol 160:64-81.
Thornton MA, Mehta MD, Morad TT, Ingraham KL, Khankan RR, Griffis KG, Yeung AK, Zhong H, Roy RR, Edgerton VR, Phelps PE (2018) Evidence of axon connectivity across a spinal cord transection in rats treated with epidural stimulation and motor training combined with olfactory ensheathing cell transplantation. Exp Neurol 309:119-133.
Thuret S, Moon LD, Gage FH (2006) Therapeutic interventions after spinal cord injury. Nat Rev Neurosci 7:628-643.
Tucker KJ, Tuncer M, Türker KS (2005) A review of the H-reflex and M-wave in the human triceps surae. Hum Mov Sci 24:667-688.
Walthers CM, Seidlits SK (2015) Gene delivery strategies to promote spinal cord repair. Biomark Insights 2015:11-29.
Warren Olanow C, Bartus RT, Baumann TL, Factor S, Boulis N, Stacy M, Turner DA, Marks W, Larson P, Starr PA, Jankovic J, Simpson R, Watts R, Guthrie B, Poston K, Henderson JM, Stern M, Baltuch G, Goetz CG, Herzog C, et al. (2015) Gene delivery of neurturin to putamen and substantia nigra in Parkinson disease: A double-blind, randomized, controlled trial. Ann Neurol 78:248-257.
Watson C, Paxinos G, Kayalioglu G (2009) The Spinal Cord: A Christopher and Dana Reeve Foundation Text and Atlas. San Diego: Elsevier.
Wenjin W, Wenchao L, Hao Z, Feng L, Yan W, Wodong S, Xianqun F, Wenlong D (2011) Electrical stimulation promotes BDNF expression in spinal cord neurons through Ca(2+)- and Erk-dependent signaling pathways. Cell Mol Neurobiol 31:459-467.
West AE, Chen WG, Dalva MB, Dolmetsch RE, Kornhauser JM, Shaywitz AJ, Takasu MA, Tao X, Greenberg ME (2001) Calcium regulation of neuronal gene expression. Proc Natl Acad Sci U S A 98:11024-11031.
Wiegert JS, Bading H (2011) Activity-dependent calcium signaling and ERK-MAP kinases in neurons: A link to structural plasticity of the nucleus and gene transcription regulation. Cell Calcium 49:296-305.
Wilson JR, Forgione N, Fehlings MG (2013) Emerging therapies for acute traumatic spinal cord injury. CMAJ 185:485-492.
Yao L, He C, Zhao Y, Wang J, Tang M, Li J, Wu Y, Ao L, Hu X (2013) Human umbilical cord blood stem cell transplantation for the treatment of chronic spinal cord injury: Electrophysiological changes and long-term efficacy. Neural Regen Res 8:397-403.
Zavalishin IA, Bochkov NP, Suslina ZA, Zakharova MN, Tarantul VZ, Naroditskiy BS, Suponeva NA, Illarioshkin SN, Shmarov MM, Logunov DY, Tutyhina IL, Verkhovskaya L V, Sedova ES, Vasiliev A V, Brylev L V, Ginzburg AL (2008) Gene therapy of amyotrophic lateral sclerosis. Bull Exp Biol Med 145:483-486.
Zhang C, Rong W, Zhang GH, Wang AH, Wu CZ, Huo XL (2018) Early electrical field stimulation prevents the loss of spinal cord anterior horn motoneurons and muscle atrophy following spinal cord injury. Neural Regen Res 13:869-876.
Zhang YT, Jin H, Wang JH, Wen LY, Yang Y, Ruan JW, Zhang SX, Ling EA, Ding Y, Zeng YS (2017) Tail nerve electrical stimulation and electro-acupuncture can protect spinal motor neurons and alleviate muscle atrophy after spinal cord transection in rats. Neural Plast 2017:7351238.
Zhong J (2016) RAS and downstream RAF-MEK and PI3K-AKT signaling in neuronal development, function and dysfunction. Biol Chem 397:215-222.
Zhu H, Poon W, Liu Y, Leung GK, Wong Y, Feng Y, Ng SCP, Tsang KS, Sun DTF, Yeung DK, Shen C, Niu F, Xu Z, Tan P, Tang S, Gao H, Cha Y, So KF, Fleischaker R, Sun D, et al. (2016) Phase I-II clinical trial assessing safety and efficacy of umbilical cord blood mononuclear cell transplant therapy of chronic complete spinal cord injury. Cell Transplant 25:1925-1943.

C-Editor: Zhao M; S-Editor: Li CH; L-Editor: Song LP; T-Editor: Jia Y